First-principles calculations of iron-hydrogen reactions in silicon

Paulo Santos,[1,a)] José Coutinho,[1] and Sven Öberg[2]
[1]*Department of Physics and I3N, University of Aveiro, Campus Santiago, 3810-193 Aveiro, Portugal*
[2]*Department of Engineering Sciences and Mathematics, Luleå University of Technology, Luleå S-97187, Sweden*

(Received 9 May 2018; accepted 13 June 2018; published online 28 June 2018)

Controlling the contamination of silicon materials by iron, especially dissolved interstitial iron (Fe_i), is a longstanding problem with recent developments and several open issues. Among these, we have the question whether hydrogen can assist iron diffusion or if significant amounts of substitutional iron (Fe_s) can be created. Using density functional calculations, we explore the structure, formation energies, binding energies, migration, and electronic levels of several FeH complexes in Si. We find that a weakly bound Fe_iH pair has a migration barrier close to that of isolated Fe_i and a donor level at $E_v + 0.5$ eV. Conversely, $Fe_iH_2(0/+)$ is estimated at $E_v + 0.33$ eV. These findings suggest that the hole trap at $E_v + 0.32$ eV obtained by capacitance measurements should be assigned to Fe_iH_2. Fe_sH-related complexes show only deep acceptor activity and are expected to have little effect on minority carrier life-time in *p*-type Si. The opposite conclusion can be drawn for *n*-type Si. We find that while in H-free material Fe_i defects have lower formation energy than Fe_s, in hydrogenated samples Fe_s-related defects become considerably more stable. This would explain the observation of an electron paramagnetic resonance signal attributed to a Fe_sH-related complex in hydrogenated Si, which was quenched from above 1000 °C to iced-water temperature. *Published by AIP Publishing.* https://doi.org/10.1063/1.5039647

I. INTRODUCTION

Iron is a fundamental constituent of many tools and industrial equipment; it is present in silicon raw materials, and that makes Fe contamination of Si ingots virtually unavoidable.[1,2] Stringent control of Fe impurities in Si is particularly critical in electronic- and solar-grade materials, as a donor level at $E_v + 0.38$ eV from interstitial iron (Fe_i)[3] leads to powerful minority carrier recombination activity in *p*-type Si,[4] most often the material of choice for the fabrication of Si solar cells.

Hydrogenation of silicon wafers has been recurrently applied in order to passivate, or at least reduce, the recombination activity from several defects and contaminants, including iron and other transition metals.[2,5–10] In Si photovoltaics, this hydrogenation process is usually accomplished by means of depositing and firing a hydrogen-soaked SiN_x layer on top of Si, which besides the surface-passivation effect also works as an anti-reflection coating for the front surface of the cell.[11,12] Other types of hydrogen introduction for passivation treatments have also been considered, including proton implantation[13] or H-plasma exposure,[14] but none is as convenient as the nitridation process.

The interaction between Fe and H in silicon has been addressed in the past. Early studies by Pearton and Tavendale[14] reported the passivation of iron- and silver-related centers in *p*-type samples exposed to hydrogen plasma. Here, the introduction of the metallic impurities was accomplished by high-temperature evaporation, and from deep-level transient spectroscopy (DLTS), the suppression of an electrical level at $E_v + 0.32$ eV, by the time connected to a Fe-O complex,[15] after the H-plasma treatment was announced as an interaction between H and Fe. No direct interaction between H and interstitial Fe (Fe_i) was reported on these studies. More than a decade later, thermally stimulated capacitance (TSCAP) measurements performed by Sadoh *et al.*[16] using iron doped floating-zone *n*-type Si that was subject to wet-etching displayed the same level, which was then reassigned to a FeH complex. Annealing studies showed that after 30-min treatments at 175 °C, the level disappeared, suggesting a low binding energy between Fe and H species. Despite these conclusions, there was no direct evidence for the presence of either Fe or H in the "$E_v + 0.32$ eV" center.

More recently, further evidence for a Fe-H complex in *p*-type silicon was reported by Leonard and co-workers.[17] Hydrogen was introduced into the samples from a silicon nitride layer grown by plasma enhanced chemical vapor deposition. After a reverse-bias annealing at about 100 °C, a hole trap was observed in the DLTS spectrum from samples with high concentrations of Fe and H. This trap was only stable up to 125 °C, and it was related to a donor level at $E_v + 0.31$ eV. The electronic signature of this trap coincided with that reported in Ref. 16.

The interaction of hydrogen with iron-related defects such as the iron-boron (FeB) pair and Fe_i itself was also addressed by Kouketsu and Isomae.[13] In this case, hydrogen was introduced by proton implantation, leading to different observations when compared to those where hydrogen plasma was used. Accordingly, along with the disappearance of the DLTS signals related to Fe_i and FeB, the emergence of two hole traps at $E_v + 0.23$ eV and $E_v + 0.38$ eV was observed. It was not clear, though, whether these new traps arose from the reaction between H and Fe_i-related complexes or, on the other hand, from complexes involving H and

a)Electronic mail: paulodsantos@ua.pt

intrinsic defects (resulting from the implantation damage), eventually combined with Fe.

The interaction of H with FeB pairs was also studied by Yakimov and Parakhonsky using wet-etching,[18] therefore avoiding implantation damage effects. Their results suggested that at room-temperature, the introduction of hydrogen actually leads to dissociation of the FeB pairs in the near surface layer, thus increasing the concentration of interstitial iron. The process leading to such dissociation is not well understood, and therefore it is worthy of further investigation.

Electron paramagnetic resonance (EPR) was also employed in the study of H-passivation of Fe in Si. Accordingly, the existence of a FeH complex with a binding energy of ~1.3 eV and stable up to $< T = 220\,^{\circ}\mathrm{C}$ was inferred after comparing EPR spectra from Fe-doped and (Fe,H)-co-doped *n*-type floating zone Si.[19] Interestingly, the EPR signal which was assigned to the FeH complex was isotropic (T_d symmetry). Unfortunately, the authors could not unambiguously demonstrate the presence of H atoms in the center, either from the EPR data or from local vibrational mode absorption using deuterated samples.

Theoretical work by the Estreicher group proposed two stable structures for the FeH complex, namely, Fe_iH and Fe_sH, involving interstitial and substitutional Fe, respectively.[20] Although under equilibrium conditions iron impurities are located at interstitial sites, there is evidence for the existence of substantial concentrations of iron substitutional (Fe_s) provided by emission channeling[21,22] and Mössbauer spectroscopy.[23–28] The Fe_iH model consists of a Fe-H dimer with trigonal symmetry, with the Fe atom placed at the hexagonal interstitial site, while H is located close to a neighboring tetrahedral interstitial site. This structure was anticipated to produce two electrical levels, a donor at $E_v + 0.36$ eV and an acceptor at $E_c - 0.26$ eV.[20] The authors also estimated an energy gain of 0.82 eV for the reaction $Fe_i + H_{BC} \rightarrow Fe_iH$ (assuming a bond-centered configuration for hydrogen and neutral defects only), consistent with the thermal stability of the '$E_v + 0.32$ eV' trap (annealing temperature of about 175 °C) as reported by Sadoh *et al.*[16] This reaction is expected to be hindered in *p*-type Si due to electrostatic repulsion between Fe_i^+ and H^+ ions.

The second structure, Fe_sH, was found to comprise an iron atom locked at a substitutional site, with the hydrogen atom roaming almost freely around it. This model was assigned to the EPR spectra reported by Takakashi and co-workers,[19] conforming to the observed isotropic symmetry. Fe_sH was predicted to produce an acceptor level at $E_c - 0.62$ eV. The estimated binding energy for this structure was approximately 1.4 eV, also in good agreement with the 1.3 eV binding energy estimated from the ESR measurements.[19] Despite the agreement, the EPR data were acquired in *n*-type material and for these conditions, the proposed Fe_sH complex would be in a diamagnetic negative charge state, raising doubts to the correctness of this assignment.

While the early literature indicates a relatively low thermal stability for Fe-H complexes (the measured binding energies and annealing experiments, on one hand,[16,17,19] and the first-principles calculations by Szwacki *et al.*,[20] on the other hand, suggest that these complexes can only survive to temperatures of at most 125–200 °C), more recently the solar-Si community has turned attention to the effect of hydrogenation on Fe diffusivity and gettering at higher temperatures. For instance, Ref. 29 reports a prominent decrease in the concentration of Fe_i after exposing multicrystalline Si wafers to a microwave-induced remote hydrogen plasma, followed by H-effusion during 300–500 °C-anneals. This is a surprisingly stable process (when compared to H-passivation using etched samples), and it was tentatively explained as a consequence of an enhanced diffusion of Fe_i caused by the introduction of H, thus leading to a faster gettering kinetics.

On the other hand, Liu *et al.*[8] questioned the picture of a H-enhanced diffusivity of Fe_i, arguing that if that was the case, any increase in the annealing temperatures should lead to the observation of further gettering of Fe. However, they report that at 700 °C, the amount of dissolved iron reaches a minimum of about 1% of the original content and recovers at higher temperatures. It was then suggested that up to 700 °C, the formation of a Fe-H complex should account for the decrease in Fe_i, and above that temperature the dissociation of the complex becomes dominant. This view was later revised after secondary-ion mass spectroscopy (SIMS) measurements combined with DLTS, annealing, and analysis of the iron-decay kinetics.[30] From the observed accumulation of Fe at the SiN_x capping layer, it was concluded that the iron reduction in the Si bulk takes place via gettering at the silicon nitride films. Hydrogenation of Fe_i at high-temperatures was ruled out based on the lack of electrical activity in the Si as monitored by DLTS. Further, upon removal of the SiN_x, subsequent high-temperature anneals did not reveal any electrical activity either.

With these observations in mind, we endeavored to calculate the stability, electrical activity, and migration ability of FeH-related complexes. After describing the methodology, we report on the atomistic structure and energetics of FeH defects, their electronic activity, thermal stability, and hydrogen-assisted migration of interstitial iron. We end up with a discussion of the results and conclusions.

II. METHOD

We employed the *Vienna Ab initio Simulation Package* (VASP) code[31–33] to perform density functional calculations concerning the relative stability, formation energies, electrical levels, and migration barriers of FeH complexes in Si. These calculations were based on the projector-augmented wave (PAW)[34] method using the generalized gradient approximated exchange-correlation functional of Perdew, Burke and Ernzerhof.[35] The PAW potentials for Fe, Si, and H species were generated in the $3s^2 3p^6 3d^7 4s^1$, $3s^2 3p^2$, and $1s^1$ valence configurations, respectively. The Kohn-Sham states were expanded in plane-waves with a cutoff energy of 450 eV.

Our atomistic models for the defects under scrutiny were inserted on 216 Si atom supercells with a theoretical lattice parameter of $a_0 = 5.456$ Å. We employed a $2 \times 2 \times 2$ Monkhorst and Pack **k**-point grid to sample the Brillouin zone.[36] The structural optimization of our defect models was done through a conjugate gradient method, with a convergence threshold of 2.5×10^{-3} eV/Å for the maximum force

acting on the nuclei. The self-consistent electronic relaxation cycles were computed with an accuracy of 10^{-7} eV.

We employed the marker method[37,38] to assess the electrical activity of the FeH complexes. The markers for the double acceptor, acceptor, and donor levels are, respectively, $Ni_s(=/-) = E_c - 0.08\,eV$, $Ni_s(-/0) = E_c - 0.31\,eV$, and $Fe_i(0/+) = E_v + 0.38\,eV$.[3,39] The respective electron affinities (A) and ionization potentials (I) calculated using the same 216-Si supercells are $A\{Ni_s(=/-)\} = 6.06\,eV$, $A\{Ni_s(-/0)\} = 5.99\,eV$, and $I\{Fe_i(0/+)\} = 5.73\,eV$. The image-charge corrections for all the markers and defects under scrutiny were accounted for using the algorithm proposed by Freysoldt, Neugebauer, and Van de Walle.[40] The marker method consists of a direct comparison between ionization potentials (or electron affinities) of the marker and that of the defect under scrutiny. While charge-corrections to the energies are of the order of hundreds of meV, these essentially cancel in the calculated electronic levels, becoming a few meV. The error bar of the calculated levels was estimated at about 0.1 eV. This figure was estimated by calculating the Fe_i and Fe_s levels, but instead of a defect marker, ionization energies and electron affinities of a bulk supercell were assumed as reference energies for the valence band top and conduction band bottom edges, respectively.

Formation energies of neutral defects, E_f^0, were determined using the following expression:

$$E_f^0 = E_{def}^0 - \sum_i n_i \mu_i, \tag{1}$$

where E_{def}^0 stands for the total energy of a neutral defective supercell made up of n_i atoms of species i with chemical potential μ_i. Chemical potentials $\mu_{Si} = -5.42$ eV, $\mu_{Fe} = -9.68\,eV$, and $\mu_H = -3.39$ eV were obtained from bulk Si, iron disilicide ($\beta-FeSi_2$), and a H_2 molecule in a box, respectively. The formation energy of a defect in charge state q has a $E_f^q \sim qE_F$ dependence, where E_F is the Fermi energy with respect to the valence band top. The calculation of E_f^q was carried out combining Eq. (1) and the results from the marker method described above. See Ref. 41 for further details.

Hydrogen-assisted migration of interstitial iron was also investigated. We employed a 7-image nudged elastic band (NEB) method[42] in order to estimate the migration/transformation barriers of FeH-related defects in the neutral and positive charge states. These are the relevant states to be considered in p-type material.

III. RESULTS

A. Defect structures

In order to determine the ground state structures of Fe_iH and Fe_sH defects, we started from the relaxed structures of Fe_i and Fe_s, respectively, and introduced one or two hydrogen atoms at several possible sites, either bonding directly to the Fe atom along different directions, next to their silicon first neighbors, at second-neighboring Si-Si bond-center sites, or near the Fe-Si bond-center site.

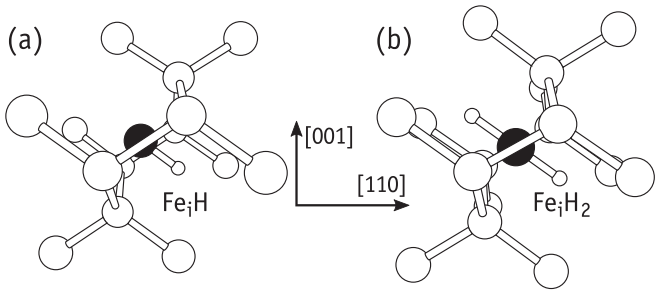

FIG. 1. Ground state structure of (a) Fe_iH and (b) Fe_iH_2 defects in silicon. The large white and black spheres and small white spheres represent Si, Fe, and H atoms, respectively. Fe-H bonds are 1.47 Å long on both defects.

In line with the calculations reported by Szwaki *et al.*,[20] we predict that after trapping one hydrogen atom, the Fe_i atom becomes more stable near the hexagonal site while connecting to H along the trigonal axis. The resulting Fe_iH structure is depicted in Fig. 1(a). The defect is stable in the negative, neutral, and positive charge states with spin 0, 1/2, and 1, respectively. The structure of the Fe_iH_2 complex is analogous, with both H atoms bonded to Fe_i pointing towards opposite directions along a common $\langle 111 \rangle$ axis. This is shown in Fig. 1(b), and the defect is also stable in the –, 0, and + charge states with spin 1/2, 1, and 1/2, respectively.

In the case of Fe_sH, we found it to be bistable, with H connecting to Fe_s along the $\langle 100 \rangle$ direction in the neutral charge state or along $\langle 111 \rangle$ towards the tetrahedral interstitial site in the negative charge state. These structures are represented in the configuration coordinate diagram of Fig. 2 and are labeled as $\{Fe_sH\}_A^0$ and $\{Fe_sH\}_B^-$, respectively. They show spin 1/2 and 0, respectively, and each of them has a unique minimum in the potential energy surface: for the

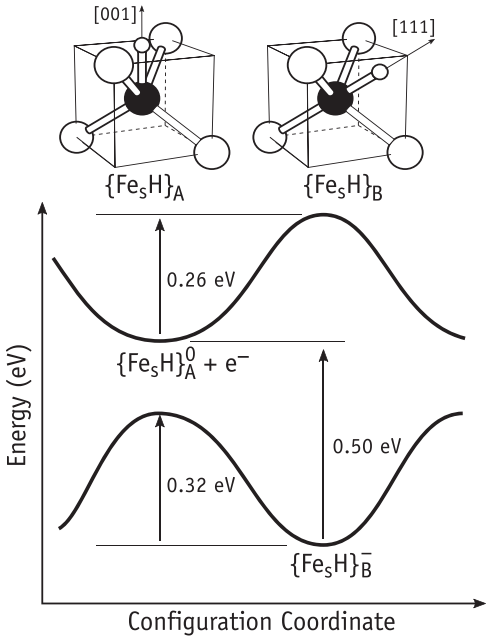

FIG. 2. Configuration coordinate diagram of the Fe_sH defect. The upper part of the figure includes the two ground-state configurations $\{Fe_sH\}_A$ and $\{Fe_sH\}_B$ for neutral and negative charge states, respectively. The black sphere represents Fe while the smaller and larger white spheres represent H and Si, respectively.

negatively charged defect, structural optimization initiated in the $\{Fe_sH\}_A$ configuration relaxed into $\{Fe_sH\}_B$. Conversely, neutral $\{Fe_sH\}_B$ is unstable and spontaneously relaxes to $\{Fe_sH\}^0_A$. The energy barriers for conversion between $\{Fe_sH\}_A \leftrightarrow \{Fe_sH\}_B$ were calculated as 0.26 eV and 0.32 eV for neutral and negative charged defects. These figures are at variance with those obtained in Ref. 20 (0.08 eV), and we can only suggest that in that work the Brillouin-zone sampling that was employed (Γ-only) was not sufficiently dense considering the size of the supercells (64 atoms).

The capture of a second hydrogen atom by Fe_s also leads to two stable Fe_sH_2 configurations in different charge states. For the neutral charge state, we obtained a linear H-Fe-H configuration with both Fe-H bonds along the ⟨100⟩ crystallographic axis, pointing towards opposite directions. This structure has high symmetry (D_{2d} point group) and from the inspection of the Kohn-Sham band structure, an empty double degenerate state in the upper half of the gap was identified. We label this structure $\{Fe_sH_2\}_A$.

In the negative charge state, the doublet state becomes partially populated and the structure undergoes a Jahn-Teller distortion. This translates into $E_{JT} \sim 0.3$ eV relaxation energy and to the formation of a slanted Fe-H bond about 10° away from the ⟨100⟩ axis. Several other low-energy distortions were found within 30 meV from the ground state. These consisted of pairs of Fe-H bonds oriented close to ⟨100⟩ and ⟨111⟩, like in $\{Fe_sH\}_A$ and $\{Fe_sH\}_B$, respectively. All non-linear H-Fe-H defects (including the ground state) were found with spin 1/2, and because they are all nearly degenerate, we refer to them as $\{Fe_sH_2\}_B$. Interestingly, the transformation barrier between these low-symmetry structures was found to be about 50 meV, indicating that the H atoms can roam almost freely around the Fe_s impurity, even at cryogenic temperatures.

In the double negative charge state, the Jahn-Teller distortion becomes stronger and both Fe_s-H bonds pointed approximately along orthogonal ⟨100⟩ directions. The resulting diamagnetic $\{Fe_sH_2\}^=_B$ state was found more stable than the paramagnetic $\{Fe_sH_2\}^=_A$ linear structure with spin-1 by 0.29 eV. The reorientation of a Fe_s-H bond now involves surmounting a barrier of 0.12 eV. All Fe-H bond lengths in Fe_sH_n defects were in the range of 1.52–1.55 Å.

Besides the electronic energy (enthalpy), at high temperatures the entropy may impact on the relative stability of defects, and here the most important contributions are from configurational and vibrational degrees of freedom. Sanati and Estreicher found that vibrational entropy can stabilize light impurities in silicon by $\sim 0.1-0.2$ eV after ramping up the temperature by up to $\Delta T = 800$ K.[43] Assuming that the magnitude of Fe-H vibrational frequencies from $\{Fe_sH\}_A$ and $\{Fe_sH\}_B$ are not very different, the vibrational entropy difference is expected to be minute. Configurational entropy is normally not considered because it is difficult to estimate analytically except for very simple structures.[44] Within the Boltzmann framework, the configurational entropy difference between structures $\{Fe_sH\}_A$ and $\{Fe_sH\}_B$ is about $k_B \ln(6/4) \approx 3.5 \times 10^{-5}$ eV/K, which translates into a mere 27 meV for $\Delta T = 800$ K. Although a detailed account of entropy effects is outside the scope of this work, the picture just presented should not be generalized, and we should bear in mind that entropy could have a stronger influence, particularly when comparing energies of defects with different stoichiometry and lattice locations.

B. Electronic levels

The donor level of interstitial iron in silicon has been experimentally determined at $E_v + 0.38$ eV.[3] We investigated the reaction of H with Fe_i in terms of the resulting electronic activity. Since Fe_i is displaced from the tetrahedral site to the hexagonal site upon bonding with one or two H atoms, the electronic activity of Fe_iH complexes is expected to differ significantly from that of isolated Fe_i. In fact, we found that besides donor activity, both Fe_iH and Fe_iH_2 complexes are acceptors. For the Fe_iH pair, we obtain $(-/0)$ and $(0/+)$ levels at $E_c - 0.22$ eV and $E_v + 0.50$ eV. On the other hand, for Fe_iH_2, we calculated $(-/0)$ and $(0/+)$ levels at $E_c - 0.29$ eV and $E_v + 0.33$ eV, respectively. No further levels were found for Fe_iH_n defects. Although our results for Fe_iH are not far from previous theoretical reports,[20] the $Fe_iH(0/+)$ level seems too deep to be connected to the "$E_v + 0.32$ eV" trap of Ref. 16. Alternatively, Fe_iH_2 shows a $(0/+)$ transition at $E_v + 0.33$ eV, i.e., about the right placement within the gap, and therefore, must be considered as potentially accountable for the above trap as well. We will come back to this issue in Sec. III D.

Now we turn to the interactions between H and substitutional iron. For $\{Fe_sH\}_A$ and $\{Fe_sH\}_B$, we obtained *vertical* $(-/0)$ transitions at $E_c - 0.18$ eV and $E_c - 0.76$ eV. However, we note that $\{Fe_sH\}^-_A$ and $\{Fe_sH\}^0_B$ are unstable, and the relevant thermodynamic acceptor level of Fe_sH must be calculated from ground state energies. Hence, we obtain $Fe_sH(-/0)$ at $E_c - 0.50$ eV (see Fig. 2). Previous first-principles calculation[20] assigned Fe_sH in the neutral charge state to an isotropic spin-1/2 EPR spectrum observed in *n*-type material at a temperature as low as 10 K.[19] The location of the $Fe_sH(-/0)$ level implies that under these conditions, the defect would be found in a diamagnetic negative charge state, and therefore undetectable by EPR. We could not find a second acceptor level for Fe_sH. Hence, the assignment of the EPR data should be revised and further work is needed to clarify this point.

For Fe_sH_2, we anticipate first and second acceptor levels at $E_c - 0.21$ eV and $E_c - 0.30$ eV, respectively. It is noteworthy that the second electron trap is deeper than the first, i.e., Fe_sH_2 shows an inverted ordering of the acceptor levels. This is commonly referred to as negative-*U* and arises from a strong relaxation energy along the capture sequence, which surmounts the Coulomb repulsion between both captured electrons. Accordingly, in the neutral charge state, Fe_sH_2 adopts structure A. This structure can capture a free-electron with a binding energy of 0.21 eV. After trapping the first electron, the structure quickly changes to $\{Fe_sH_2\}_B$, where some of the relaxation energy is effectively converted to an increase in the Coulomb attraction for the second electron, leading to a binding energy of 0.30 eV. The consequence of the negative-*U* ordering of levels is that, under equilibrium conditions, it is energetically favorable to form a pair of $\{Fe_sH_2\}^0$ and

TABLE I. Calculated electrical levels for Fe_iH_n and Fe_sH_n complexes. All reported values are in eV. The inverted order of levels for Fe_sH_2 leads to a $(=/0)$ occupancy level at $E_c - 0.26$ eV (see the text).

	$E_c - E(=/-)$	$E_c - E(-/0)$	$E(0/+) - E_v$
Fe_iH		0.22	0.50
Fe_iH_2		0.29	0.33
Fe_sH		0.50	
Fe_sH_2	0.30	0.21	

$\{Fe_sH_2\}^=$ states than two $\{Fe_sH_2\}^-$ structures (irrespectively of the Fermi level position). Hence, Fe_sH_2 has an $(=/0)$ occupancy level that is located half-way between the first and second acceptor levels, i.e., $Fe_sH_2(=/0) = E_c - 0.26$ eV. All calculated electrical levels are shown in Table I.

C. Binding energies and doping effects

The diagrams presented in Fig. 3 show the formation energies of several defect sets involving one Fe_i impurity plus two interstitial H atoms (left), in comparison with one Fe_s impurity plus two interstitial H atoms (right) as a function of the Fermi energy. On each diagram the stoichiometry is conserved. The formation energy (vertical) scales are identical for a convenient comparison. Each sequence of connected segments relates to a particular set involving a Fe_iH_n or Fe_sH_n complex plus $2-n$ remote interstitial H atoms. The formation energy is proportional to qE_F, with q and E_F being the net charge of the whole defect set and Fermi level, respectively. Hence, positive-, zero-, and negative-sloped segments refer to defect sets with net positive, neutral, and negative charge, respectively. For instance, for Fe_iH plus a remote H atom (on the left diagram), as the Fermi energy goes from the valence band top ($E_F = 0$) to the conduction band bottom ($E_F = 1.17$ eV), the sequence is $\{Fe_iH\}^+ + H_{BC}^+$ (net charge $q = +2$); $\{Fe_iH\}^0 + H_{BC}^+$ (net charge $q = +1$); $\{Fe_iH\}^0 + H_T^-$ (net charge $q = -1$); $\{Fe_iH\}^- + H_T^-$ (net charge $q = -2$). Hence, each kink between adjacent segments corresponds to a particular transition level identified in the figure. We note that transition levels of Fe_i and interstitial H are measured. The latter is a negative-U defect with donor and acceptor levels at $E_c - 0.18$ eV and $E_c - 0.5$ eV, leading to a $(-/+)$ occupancy level at $E_c - 0.34$ eV.[45–48] Positive and negatively charged H defects are more stable at the bond-center (H_{BC}^+) and tetrahedral interstitial sites (H_{BC}^-), respectively. The neutral charge state [used to calculate the formation energy in Eq. (1)] was found more stable in the bond-center site (H_{BC}^0). Experimental and calculated levels are highlighted by open and closed circles on both diagrams. Finally, on the diagram related to Fe_sH_n defects, we made use of color to distinguish A and B structures of Fe_sH and Fe_sH_2 complexes.

Looking at the diagram on the left-hand side of Fig. 3, we conclude that the capture of atomic H by Fe_i is an energetically favorable process regardless of the Fermi level position. The energy drop of the formation energy as we move from the upper segments ($Fe_i + 2H$) down to the lower segments (Fe_iH_2) represents the binding energy of the reaction $H + Fe_iH_n \rightarrow Fe_iH_{n+1}$, with $n = 0$ or 1. In intrinsic material (considering the Fermi level to be approximately at mid-gap), the capture of H by Fe_i corresponds to an energy gain of $\sim$0.56 eV. The capture of a second hydrogen atom corresponds to an energy gain of $\sim$0.80 eV, leading to a total binding energy of $\sim$1.36 eV to form a neutral Fe_iH_2 complex. In p-type materials, these reactions become less exothermic and the formation of Fe_iH_n complexes becomes less likely. Hydrogenation of Fe_i is further hindered in p-type Si due to the fact that both H and Fe_iH_n complexes are deep donors, implying a long-range Coulomb repulsion between reactants. On the other hand, in n-type Si there is no Coulomb barrier for the reaction $Fe_i^0 + H_T^- \rightarrow Fe_iH^-$ and the energy drop is $\sim$0.6 eV. The reaction with a second hydrogen atom has a binding energy of 0.75 eV, but it is likely to be inhibited by repulsion between H_T^- and $\{Fe_sH\}^-$. In summary, hydrogenation of interstitial iron in Si leads to Fe_iH_n complexes whose binding energies are low, and they are compatible with the annealing temperature of 125–175 °C of the FeH-related complex reported in Refs. 16 and 17.

The diagram on the right-hand side of Fig. 3 immediately suggests that H binds strongly to Fe_s, regardless of the doping type. In n-type Si, the binding energies are $\sim$1.4 eV, in excellent agreement with the measured binding energy of 1.3 eV for a FeH-related complex in n-type Si, where Fe was suggested to be at the substitutional site.[19] In the lower part of the right diagram, we also represent the formation energy of the negatively charged $\{Fe_sH_2\}_B^-$, just above the $Fe_sH_2(=/0)$ negative-U transition at $E_c - 0.26$ eV. This is shown as a dashed line to stress its metastable character.

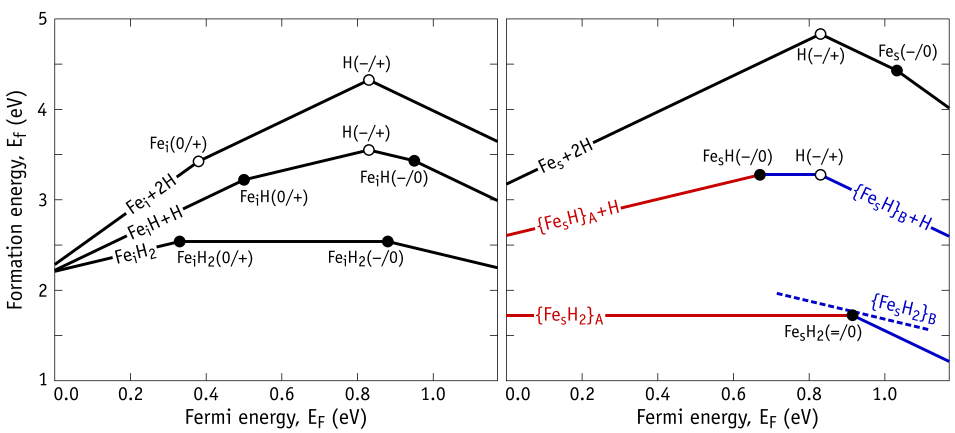

FIG. 3. Diagrams with the formation energy (E_f) as a function of the Fermi energy (E_F) for different defect arrangements involving the hydrogenation of Fe_i (left) and Fe_s (right) defects. Open and closed circles highlight experimental and calculated electronic levels. Colors on the right diagram are used to clarify A (red) and B (blue) structures of Fe_sH and Fe_sH_2 complexes. See text at the beginning of Sec. III C for further details.

A more judicious inspection of Fig. 3 allows us to conclude that, while in hydrogen-free material iron impurities have a lower formation energy at the interstitial site, in H-doped Si, the lower formation energy complexes are those involving substitutional iron. This suggests that even in *p*-type Si, high temperature anneals (maybe with optical excitation in order to avoid Coulomb repulsion by changing the charge state of either H or Fe impurities) may be able to convert highly mobile and recombination active Fe_i impurities into stable and low-recombination active Fe_s impurities, where H atoms act as catalysts. Although we are not the first to realize this possibility,[20] it lacked theoretical support and it has been overlooked by the solar-Si community.

D. H-assisted diffusivity of iron

Bearing in mind the observation of the enhancement of Fe-gettering upon introduction of hydrogen (see, for instance, Refs. 8, 29, and 30), and considering the high thermal stability of the species (or phase) holding the Fe (which survives to temperatures above 500 °C), we investigated an eventual enhanced migration of Fe_i assisted by H. This could lead to a faster formation of iron precipitates or out-diffusion from the Si. For Fe_i, we considered a simple interstitial mechanism through the hexagonal site. In the case of Fe_iH, the defect was found to travel as a molecule, also through neighboring hexagonal sites. As we mentioned before, a total of 7 NEB images were considered in order to determine the saddle point along the minimum energy path. The calculated migration barriers are 0.50 eV, 0.65 eV, and 0.61 eV for Fe_i^+, $\{Fe_iH\}^0$, and $\{Fe_iH\}^+$, respectively. The barrier for migration of Fe_i^+ is in very good agreement with the measurements, which is about 0.6 eV (see Ref. 4 and references therein). Both $\{Fe_iH\}^0$ and $\{Fe_iH\}^+$ have migration barriers comparable to that of interstitial iron, and in p-type Si, they are considerably larger than the binding energy of H to Fe_i. These results suggest that hydrogen, if able to attach to Fe_i, does not enhance its diffusivity.

IV. DISCUSSION AND CONCLUSIONS

We calculated the structure, formation energies, binding energies, and electronic levels of several FeH complexes in Si. Fe_iH and Fe_iH_2 defects consist of Fe-H and H-Fe-H pseudo-molecules, respectively, with the Fe and H atoms being located close to hexagonal and tetrahedral interstitial sites of the lattice. The modest binding energies of the H atoms to Fe_i seem consistent with the annealing temperature in the range of 125–175 °C reported for a hole trap at $E_v + 0.32$ eV and assigned to an iron-hydrogen complex.[16,17,20] However, an assignment to Fe_iH (with a single H atom) conflicts with its predicted migration barrier, which is close to that of Fe_i. Accordingly, both defects are expected to anneal out at close temperatures (just above room temperature). For the same reasons, Fe_iH complexes are not able to account for the reduction of Fe_i upon annealing hydrogenated multicrystalline wafers in the temperature range of 700–900 °C.[8,29,30]

Fe_iH and Fe_iH_2 complexes were predicted to be simultaneously deep donors and acceptors, and therefore are not expected to substantially decrease the recombination activity of Fe in Si. The calculated levels and binding energies suggest that the donor level measured at $E_v + 0.32$ eV from Refs. 16 and 17 is likely to arise from a Fe_iH_n complex involving 2 or more H atoms. The $Fe_iH_2(0/+)$ transition is predicted at $E_v + 0.33$ eV, while $Fe_iH(0/+)$ is anticipated to occur close to mid-gap.

Substitutional iron and Fe_sH_n complexes are acceptors. No donor levels were found for these defects. For the Fe_sH pair, we obtain a single acceptor level close to mid-gap. While this result is in line with Ref. 20, it is not regarding the calculated barrier for H motion around the Fe_s impurity. In that work, the barrier was estimated to be as low as 0.08 eV, allowing the assignment of neutral Fe_sH to an isotropic EPR center observed in *n*-type Si.[19] Our results do not corroborate this view. The calculated barrier for Fe-H bond reorientation is anticipated to be as high as 0.26 eV, which is not compatible with a *fast-orbiting* H atom and a motional-averaged tetrahedral symmetry at $T = 10$ K. Further, the near mid-gap location of the calculated $Fe_sH(-/0)$ deep acceptor means that in *n*-type material the stable state is diamagnetic Fe_sH^- (undetectable by EPR).

Regarding Fe_sH_2, we found a ⟨100⟩-aligned H-Fe-H linear structure in the neutral charge state. The point symmetry of the defect is D_{2d}, and it has an empty doublet in the gap. Negative and double negative charge states are sensitive to Jahn-Teller distortions. The negatively charged defect is particularly interesting as it shows several possible low energy configurations with different angles between Fe-H bonds, differing by at most 30 meV in their relative energy and separated by reorientation barriers as shallow as 50 meV. Based on these findings, we suggest that the FeH-related EPR signal from Ref. 19 arises from $Fe_sH_2^-$ or other Fe_sH_n complex with $n > 2$. The latter option is perhaps the most probable as Fe_sH_2 is a negative-*U* complex with a metastable negative state (see the dashed line segment on the right diagram of Fig. 3).

Figure 3 shows that the formation energy of Fe_i in non-hydrogenated Si is lower than that of Fe_s by about 0.5 eV. This explains the preference of iron to occupy interstitial sites. However, in the presence of hydrogen, the formation of Fe_s-related complexes becomes favorable. This could explain the formation of large amounts of Fe_s H-related defects in hydrogenated Si, as detected by EPR after quenching the samples from 950 to 1250 °C to 0 °C.[19]

ACKNOWLEDGMENTS

This work was funded by the Fundação para a Ciência e a Tecnologia (FCT) under Project Nos. PTDC/CTM-ENE/1973/2012 and UID/CTM/50025/2013, and funded by FEDER funds through the COMPETE 2020 Program. Computer resources were provided by the Swedish National Infrastructure for Computing (SNIC) at PDC.

[1]L. Jastrzebski, J. Lagowski, W. Henley, and P. Edelman, MRS Proc. **354**, 405 (1994).
[2]A. A. Istratov, H. Hieslmair, and E. R. Weber, Appl. Phys. A **70**, 489 (2000).

[3]H. Feichtinger, J. Waltl, and A. Gschwandtner, Solid State Commun. **27**, 867 (1978).
[4]A. A. Istratov, H. Hieslmair, and E. R. Weber, Appl. Phys. A **69**, 13 (1999).
[5]S. J. Pearton and A. J. Tavendale, Phys. Rev. B **26**, 7105 (1982).
[6]R. Singh, S. J. Fonash, and A. Rohatgi, Appl. Phys. Lett. **49**, 800 (1986).
[7]A. R. Peaker, V. P. Markevich, B. Hamilton, G. Parada, A. Dudas, A. Pap, E. Don, B. Lim, J. Schmidt, L. Yu, Y. Yoon, and G. Rozgonyi, Phys. Status Solidi A **209**, 1884 (2012).
[8]A. Liu, C. Sun, and D. Macdonald, J. Appl. Phys. **116**, 194902 (2014).
[9]L. Scheffler, V. Kolkovsky, and J. Weber, J. Appl. Phys. **117**, 085707 (2015).
[10]J. Mullins, S. Leonard, V. P. Markevich, I. D. Hawkins, P. Santos, J. Coutinho, A. G. Marinopoulos, J. D. Murphy, M. P. Halsall, and A. R. Peaker, Phys. Status Solidi A **214**, 1700304 (2017).
[11]F. Jiang, M. Stavola, A. Rohatgi, D. Kim, J. Holt, H. Atwater, and J. Kalejs, Appl. Phys. Lett. **83**, 931 (2003).
[12]J. K. Holt, D. G. Goodwin, A. M. Gabor, F. Jiang, M. Stavola, and H. A. Atwater, Thin Solid Films **430**, 37 (2003).
[13]M. Kouketsu and S. Isomae, J. Appl. Phys. **80**, 1485 (1996).
[14]S. J. Pearton and A. J. Tavendale, J. Phys. C: Solid State Phys. **17**, 6701 (1984).
[15]K. Wünstel and P. Wagner, Solid State Commun. **40**, 797 (1981).
[16]T. Sadoh, K. Tsukamoto, A. Baba, D. Bai, A. Kenjo, T. Tsurushima, H. Mori, and H. Nakashima, J. Appl. Phys. **82**, 3828 (1997).
[17]S. Leonard, V. P. Markevich, A. R. Peaker, B. Hamilton, and J. D. Murphy, Appl. Phys. Lett. **107**, 032103 (2015).
[18]E. B. Yakimov and A. L. Parakhonsky, Solid State Phenom. **57–58**, 383 (1997).
[19]T. Takahashi and M. Suezawa, Phys. B: Condens. Matter **273–274**, 445 (1999).
[20]N. G. Szwacki, M. Sanati, and S. K. Estreicher, Phys. Rev. B **78**, 113202 (2008).
[21]U. Wahl, J. G. Correia, E. Rita, J. P. Araújo, J. C. Soares, and ISOLDE Collaboration, Phys. Rev. B **72**, 014115 (2005).
[22]D. J. Silva, U. Wahl, J. G. Correia, and J. P. Araújo, J. Appl. Phys. **114**, 103503 (2013).
[23]D. Gilles, W. Schröter, and W. Bergholz, Phys. Rev. B **41**, 5770 (1990).
[24]G. Langouche, Hyperfine Interact. **72**, 215 (1992).
[25]G. Weyer, S. Degroote, M. Fanciulli, V. N. Fedoseyev, G. Langouche, V. I. Mishin, A.-M. V. Bavel, A. Vantomme, and ISOLDE Collaboration, in *Defects in Semiconductors 19*, Materials science forum (Trans Tech Publications, 1997), Vol. 258, pp. 437–442.
[26]G. Weyer, A. Burchard, M. Fanciulli, V. N. Fedoseyev, H. P. Gunnlaugsson, V. I. Mishin, and R. Sielemann, Phys. B: Condens. Matter **273**, 363 (1999).
[27]Y. Yoshida, Y. Kobayashi, A. Yoshida, X. Diao, S. Ogawa, K. Hayakawa, K. Yukihira, F. Shimura, and F. Ambe, Hyperfine Interact. **141**, 157 (2002).
[28]Y. Yoshida, S. Ogawa, and K. Arikawa, Phys. B: Condens. Matter **340**, 605 (2003).
[29]P. Karzel, A. Frey, S. Fritz, and G. Hahn, J. Appl. Phys. **113**, 114903 (2013).
[30]A. Y. Liu, C. Sun, V. P. Markevich, A. R. Peaker, J. D. Murphy, and D. Macdonald, J. Appl. Phys. **120**, 193103 (2016).
[31]G. Kresse and J. Hafner, Phys. Rev. B. **47**, 558 (1993).
[32]G. Kresse and J. Hafner, Phys. Rev. B **49**, 14251 (1994).
[33]G. Kresse and J. Furthmüller, Phys. Rev. B **54**, 11169 (1996).
[34]P. E. Blöchl, Phys. Rev. B **50**, 17953 (1994).
[35]J. P. Perdew, K. Burke, and M. Ernzerhof, Phys. Rev. Lett. **77**, 3865 (1996).
[36]H. J. Monkhorst and J. D. Pack, Phys. Rev. B **13**, 5188 (1976).
[37]A. Resende, R. Jones, S. Öberg, and P. R. Briddon, Phys. Rev. Lett. **82**, 2111 (1999).
[38]J. Coutinho, V. J. B. Torres, R. Jones, and P. R. Briddon, Phys. Rev. B **67**, 035205 (2003).
[39]M. Shiraishi, J.-U. Sachse, H. Lemke, and J. Weber, Mater. Sci. Eng. B **58**, 130 (1999).
[40]C. Freysoldt, J. Neugebauer, and C. G. V. de Walle, Phys. Rev. Lett. **102**, 016402 (2009).
[41]J. Coutinho, V. P. Markevich, A. R. Peaker, B. Hamilton, S. B. Lastovskii, L. I. Murin, B. J. Svensson, M. J. Rayson, and P. R. Briddon, Phys. Rev. B **86**, 174101 (2012).
[42]G. Henkelman, B. P. Uberuaga, and H. Jónsson, J. Chem. Phys. **113**, 9901 (2000).
[43]M. Sanati and S. K. Estreicher, Solid State Commun. **128**, 181 (2003).
[44]S. K. Estreicher, M. Sanati, D. West, and F. Ruymgaart, Phys. Rev. B **70**, 125209 (2004).
[45]B. Holm, K. B. Nielsen, and B. B. Nielsen, Phys. Rev. Lett. **66**, 2360 (1991).
[46]N. Johnson, C. Herring, and C. V. de Walle, Phys. Rev. Lett. **74**, 1889 (1995).
[47]K. B. Nielsen, B. B. Nielsen, J. Hansen, E. Andersen, and J. U. Andersen, Phys. Rev. B **60**, 1716 (1999).
[48]K. B. Nielsen, L. Dobaczewski, S. Søgård, and B. B. Nielsen, Phys. Rev. B **65**, 075205 (2002).